CellPress

Developmental Cell
Article

Regulation of Plant Stem Cell Quiescence by a Brassinosteroid Signaling Module

Josep Vilarrasa-Blasi,[1] Mary-Paz González-García,[1] David Frigola,[2] Norma Fàbregas,[1] Konstantinos G. Alexiou,[1] Nuria López-Bigas,[3] Susana Rivas,[4,5] Alain Jauneau,[6] Jan U. Lohmann,[7] Philip N. Benfey,[8] Marta Ibañes,[2] and Ana I. Caño-Delgado[1,*]

[1]Department of Molecular Genetics, Center for Research in Agricultural Genomics (CRAG) CSIC-IRTA-UAB-UB, Campus UAB, Bellaterra (Cerdanyola del Vallès), 08193 Barcelona, Spain
[2]Departament d'Estructura i Constituents de la Matèria, Facultat de Física, Universitat de Barcelona, 08028 Barcelona, Spain
[3]Biomedical Genomic Group, Research Unit on Biomedical Informatics (GRIB), Barcelona Biomedical Research park (PRBB), Dr. Aiguader 88, 08003 Barcelona, Spain
[4]INRA, Laboratoire des Interactions Plantes-Microorganismes (LIPM), UMR441, 31326 Castanet-Tolosan, France
[5]CNRS, Laboratoire des Interactions Plantes-Microorganismes (LIPM), UMR2594, 31326 Castanet-Tolosan, France
[6]Fédération de Recherche 3450, Plateforme Imagerie, Pôle de Biotechnologie Végétale, 31320 Castanet-Tolosan, France
[7]Center for Organismal Studies (COS), University of Heidelberg, 69120 Heidelberg, Germany
[8]Department of Biology, HHMI and Duke Center for Systems Biology, Duke University, Durham, NC 27708, USA
*Correspondence: ana.cano@cragenomica.es
http://dx.doi.org/10.1016/j.devcel.2014.05.020

SUMMARY

The quiescent center (QC) maintains the activity of the surrounding stem cells within the root stem cell niche, yet specific molecular players sustaining the low rate of QC cell division remain poorly understood. Here, we identified a R2R3-MYB transcription factor, *BRAVO (BRASSINOSTEROIDS AT VASCULAR AND ORGANIZING CENTER),* acting as a cell-specific repressor of QC divisions in the primary root of *Arabidopsis*. Ectopic BRAVO expression restricts overall root growth and ceases root regeneration upon damage of the stem cells, demonstrating the role of BRAVO in counteracting Brassinosteroid (BR)-mediated cell division in the QC cells. Interestingly, BR-regulated transcription factor BES1 (BRI1-EMS SUPRESSOR 1) directly represses and physically interacts with BRAVO in vivo, creating a switch that modulates QC divisions at the root stem cell niche. Together, our results define a mechanism for BR-mediated regulation of stem cell quiescence in plants.

INTRODUCTION

Cellular quiescence is a temporary and reversible cell cycle arrest characterized by programmed events that avoid proliferation. However, in eukaryotes, little is known about the molecular determinants for the quiescent state (Cheung and Rando, 2013). Self-renewal of quiescent cells acts as a replenishment source, e.g., in the hematopoietic case it ensures long-term maintenance of multipotent stem cells throughout the organismal lifespan (Wilson and Trumpp, 2006). In plants, the root stem cell niche is composed of different sets of stem cells that give rise to specific root cell lineages, which are surrounding a group of cells with low proliferation rate termed quiescent center (QC) (Scheres, 2007; Figure 1A). The QC cells maintain the stemness of neighboring cells, which function as a major signaling hub maintaining the proliferation/differentiation rates (Cheung and Rando, 2013; Scheres, 2007), where retinoblastoma (RBR) plays an autonomous control in the regulation of QC division (Wachsman et al., 2011). The proper balance between quiescence and proliferation ensures organismal longevity and prevents both genetic damage and stem cell exhaustion (Cheung and Rando, 2013).

Plant steroid hormones, Brassinosteroids (BRs), are essential regulators of plant architecture, growth and development. BR perception through the plasma membrane-localized BRASSINOSTEROID INSENSITIVE 1 (BRI; Li and Chory, 1997), a leucine-rich-repeat receptor-like-kinase (LRR-RKL) protein promoting the translocation of BRI1 EMS SUPPRESSOR 1 (BES1) and BRASSINAZOLE-RESISTANT 1 (BZR1; Wang et al., 2002; Yin et al., 2002) to the nucleus where they regulate gene expression (Sun et al., 2010; Yu et al., 2011). Despite the high degree of knowledge regarding BR-signaling components, how the regulatory events downstream of BES1 and BZR1 are translated into specific developmental outputs remains poorly understood.

The local action of BRs in stomata patterning and establishment of organ boundary (Bell et al., 2012; Gendron et al., 2012; Gudesblat et al., 2012; Kim et al., 2012) argues for cell-specific BR pathways in different organs. However, the majority of the BR signaling components are ubiquitously expressed in the plant, yet cell-specific components have not been identified. In the primary root, BRs are essential regulators of growth and development (Fàbregas et al., 2013; González-García et al., 2011; Hacham et al., 2011; Müssig et al., 2003). BRs promote the division of QC cells at the root stem cell niche, suggesting that counteracting BR signaling is a mechanism to preserve the low rates of cell division in the QC (González-García et al., 2011; Heyman et al., 2013); however, cell-specific repressors of the BR pathway remain to be identified.

In this study, we used a cell-based transcriptomic approach to identify cell-specific regulators of the BR-mediated signaling in

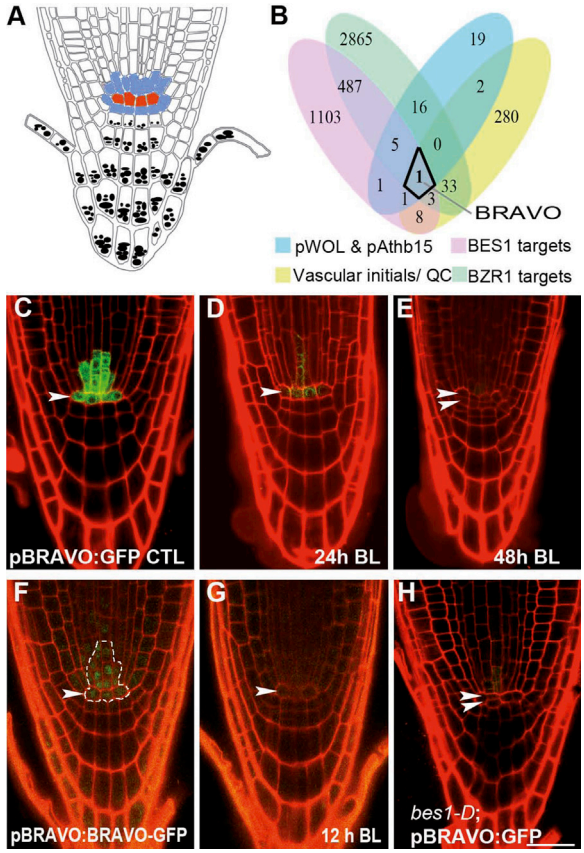

Figure 1. *BRAVO* Encodes a R2R3-MYB Transcription Factor Directly Regulated by BR-Regulated BES1 in the Vascular Initials and the QC Cells

(A) Schematic representation of the root stem cell niche in *Arabidopsis thaliana* (*Arabidopsis*) stem cells (blue) surrounds QC cells (red).

(B) Venn diagram of the deregulated transcription factors in *pWOL:GFP* and *pAthb15:YFP*, enriched in the vascular initials/QC together with BES1 and BZR1 targets; only one gene fit all criteria, i.e., *BRAVO*.

(C–H) Six-day-old seedlings counterstained with propidium iodide (PI).

(C) Expression of *pBRAVO:GFP* is restricted to the vascular initials and the QC cells

(D and E) BL treatment of *pBRAVO:GFP*, 24 and 48 hr, respectively, promotes BRAVO repression.

(F and G) *BRAVO* a nuclear transcription factor repressed after BL application.

(H) Reduction of *pBRAVO:GFP* expression in the *bes1-D* mutant background. White arrows represent QC cells.

Scale bar in (C–H) represent 25μm. See also Figures S1 and S2.

the root stem cell niche. We report the identification of a R2R3-MYB transcription factor, *BRAVO (BRASSINOSTEROIDS AT VASCULAR AND ORGANIZING CENTER),* acting as cell-specific repressor of BR-mediated divisions in the stem cell niche of the *Arabidopsis* root. *BRAVO* mutant plants show strong dividing QCs, whereas BRAVO overexpression under an inducible promoter represses root growth, leading to root growth exhaustion upon genotoxic stress. BES1 directly represses and physically interacts with BRAVO in vivo, enabling strong BRAVO expression in QC cells and null or low BES1 signaling, which together ensure quiescence. In addition, the BR-activated BES1 signaling drives an ultrasensitive response toward the repression of BRAVO, thereby promoting QC divisions at the root stem cell niche. Our study reveals that the BRAVO/BES1 signaling module defines a mechanism for BR-mediated regulation of stem cell quiescence in plants.

RESULTS

BRAVO Defines a BR-Regulated Transcription Factor Specific to Root Stem Cells

To identify cell-specific BR-signaling components, the primary roots of the stele marker *WOODEN LEG* (Mähönen et al., 2000; *pWOL:GFP*) were treated with 10 nM Brassinolide (BL, the most active BR compound) at 0.5, 1, 2, and 4 hr (Figure S1 available online). The stele cells were isolated with fluorescent-activated cell sorting (FACS) of green fluorescent protein (GFP) marked cells and subjected to microarray analysis (Birnbaum et al., 2005), revealing a total of 309 significantly differentially regulated genes (fold change > 1.5; $p < 0.01$; see Experimental Procedures; Table S2). Time-course analysis showed a peak of 120 deregulated genes after 2 hr BL treatment (Figure S1), whereas gene ontology (GO) enrichment analysis (López-Bigas et al., 2008) disclosed cell cycle, histone modification, gravitropism, and phloem/xylem histogenesis among the most enriched categories (Figure S1). To further refine our search, we used the *CORONA/ATHB15* (Zhiponova et al., 2013; *pAthb15:YFP*) marker that labels a few provascular meristematic cells (Figure S1) to perform FACS and microarray analysis after 2 hr of BL treatment (724 genes, fold change > 1.5; $p < 0.01$; Table S2). The differentially expressed genes were then compared with both BES1 and BZR1 direct targets (Sun et al., 2010; Yu et al., 2011) to identify cell-specific regulators. Venn-diagram comparison of these genes with a set of vascular initial/quiescent center (QC) enriched genes (Brady et al., 2007; Nawy et al., 2005) identified a single gene that matched all criteria (Figure 1B). The gene corresponds to an R2R3-MYB transcription factor, MYB56 (At5g17800), hereafter renamed *BRAVO* (*BRASSINOSTEROIDS AT VASCULAR AND ORGANIZING CENTER*).

In agreement with the microarray data, *BRAVO* expression *(pBRAVO:GFP)* appeared to be specific to vascular initial and QC cells of the root apical meristem (Figure 1C). *BRAVO* transcription was specifically downregulated by BRs in a dose- and time-dependent manner (Figures 1D and 1E; Figure S2). Exogenous treatments with different plant hormones such as abscisic acid, gibberelins, and ethylene previously related to root stem-cell maintenance failed to significantly modify BRAVO expression in short-term applications (Figure S2). Similarly, BRAVO protein (*pBRAVO:BRAVO-GFP*) was localized at the nuclei of vascular initials and QC cells and disappeared rapidly upon short-term BL treatment (Figures 1F and 1G). The BR-activated *bes1-D* mutant that accumulates the active (dephosphorylated) form of BES1 (Yin et al., 2002) exhibited a dramatic reduction in *BRAVO* levels (Figures 1C and 1H; Figure S2). Collectively, these results show that the *BRAVO* locus defines a cell-specific component of the BR signaling pathway at the root stem cell niche of *Arabidopsis*.

BRAVO Is a Negative Regulator of QC Divisions

Previous analyses established that BR-activated BRI1 and BES1 signaling promotes the division of QC cells in the root stem cell

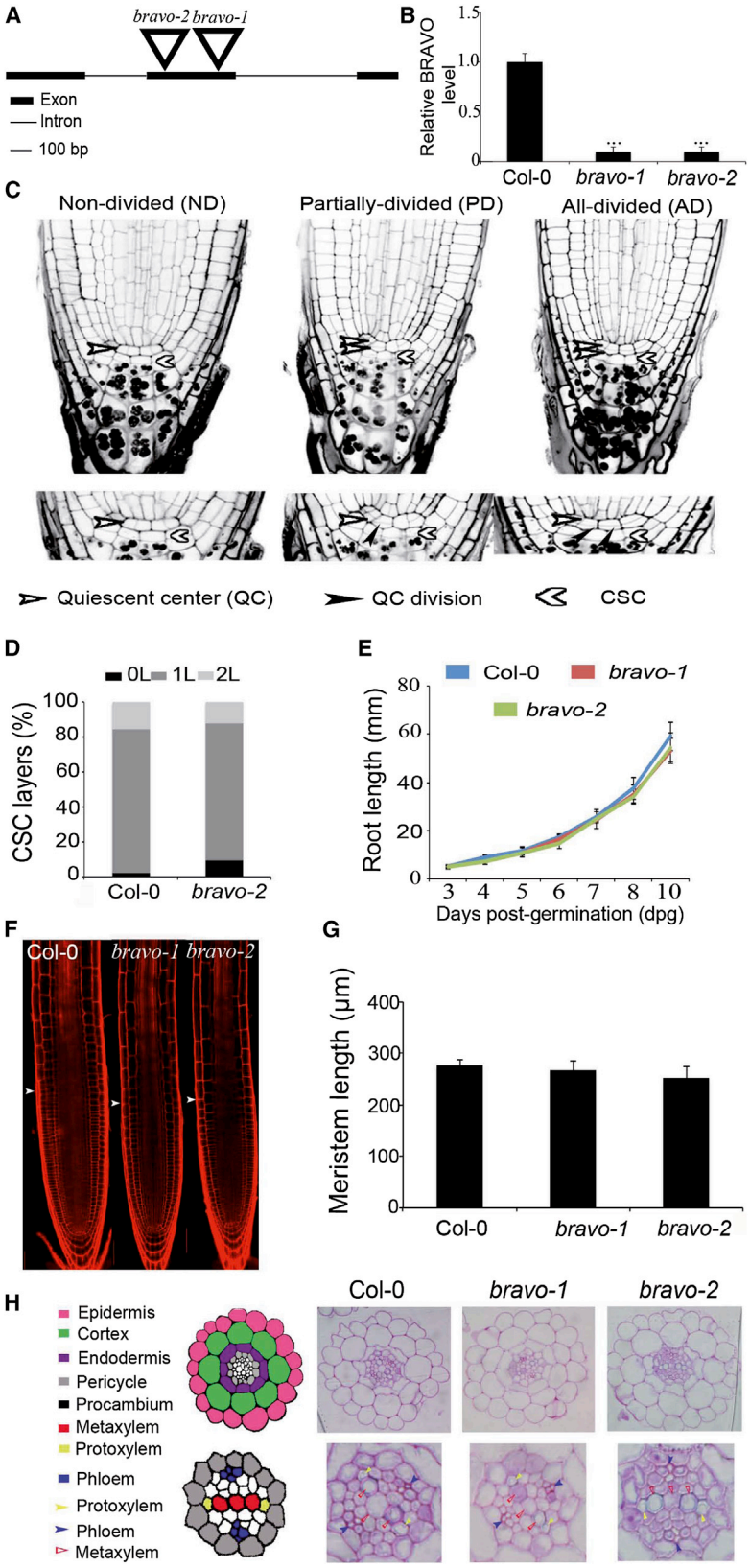

Figure 2. Phenotypic Analysis of *bravo* Mutants in the Primary Root

(A) Schematic representation of *BRAVO* gene with the T-DNA insertions in the second exon of the gene.

(B) Relative *BRAVO* levels in *bravo-1* and *bravo-2* mutant alleles.

(C) Six-day-old seedlings mPS-PI stained of *bravo* mutants. White arrows indicate QC position and black arrows the position of QC-divided cells.

(D) Quantification of columella stem cell layers.

(E) Root length of Col-0, *bravo-1*, and *bravo-2*.

(F) Six-day-old roots counterstained with PI, white arrow indicates the end of meristematic cells.

(G) Quantification of meristem length of Col-0, *bravo-1*, and *bravo-2*.

(H) Transverse root sections of 6-day-old col-0, *bravo-1*, and *bravo-2* seedlings stained with toluidine blue.

***$p < 0.005$. Error bars ± SEM.

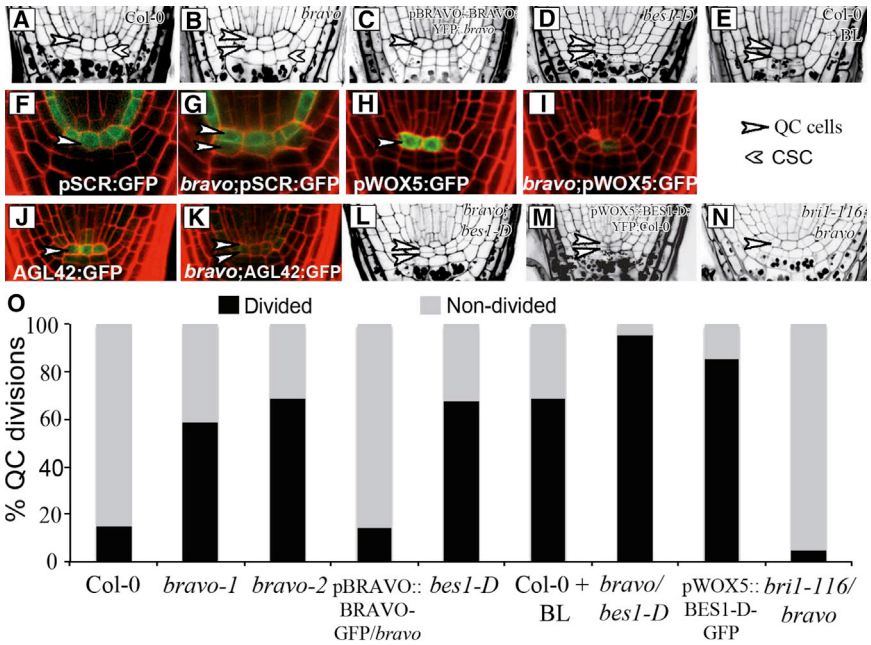

Figure 3. *BRAVO* Controls QC Divisions

(A–E, L–N) Microscopy images of mPS-PI stained 6-day-old roots with indicated genotypes, Brassinolide (BL, 0.004 nM).

(F–K) Six-day-old seedlings counterstained with PI; (F) *pSCR:GFP*, (G) *bravo/pSCR:GFP*, (H) *pWOX5:GFP*, (I) *bravo/pWOX5:GFP*, (J) *AGL42-GFP* and (K) *bravo/AGL42-GFP*.

(O) Quantification of the QC divisions in 6-day-old roots expressed in percentage, (n > 50 seedlings for each genotype, see Table S1).

See also Figure S3.

niche (González-García et al., 2011), yet the mechanism for such regulation is not known. To determine whether the BR-signaling component BRAVO controls QC divisions, we analyzed loss-of-function *bravo* mutants in the primary root apex (Figure 2). Six-day-old seedlings were analyzed for two independent knockout T-DNA insertion lines (Figures 2A and 2B). Unless for the increased QC divisions (Figure 2C), the *bravo* mutants did not show apparent phenotypes observed in root growth and development (Figures 2D–2I). Microscopic analysis revealed an ~3-fold increase in the frequency of QC divisions in *bravo* mutants as compared to wild-type (WT; 70% versus 15%; N > 100 for each genotype), and this was restored to the WT levels in *pBRAVO:BRAVO-YFP*; *bravo* plants (Figures 3A–3C, 3O; Table S1). Moreover, the additionally divided cells of *bravo* mutants express the QC and endodermis identity marker *SCARECROW* (*SCR*; Sabatini et al., 2003; Figures 3F and 3G). A progressive fade-out of SCR expression over time in the newly rootward QC cell indicates an asymmetric QC division (Figures 2F and 2G, Figure S3), in agreement with previously published work (Wachsman et al., 2011). Furthermore, QC markers *WOX5* (Sarkar et al., 2007) and *AGL42* (Nawy et al., 2005) were also present in the divided QC cells of *bravo* mutants (Figures 3H–3K, Figure S3), yet their expression appeared to be below WT levels.

BRAVO loss-of-function mutant phenotype resembles that of plants with excess of BR signaling, such as the gain-of-function *bes1-D* (70%) and plants exogenously treated with BL (0.04 nM; 70%; Figures 3D, 3E, and 3O). In agreement, the additional QC divisions observed in plants with excess of BRs appeared concomitantly with *BRAVO* downregulation (Figures 1E and 1H). In contrast to the *bes1-D,* the *bravo* mutants did not exhibit defects in neither distal nor proximal stem cell differentiation (Figures 2C, 2D, 3A, 3B, and 3D), indicating that *BRAVO* specifically functions as a local repressor of QC self-renewal in the primary root.

Next, we investigated whether QC divisions are downstream of BES1 and BZR1 in the BR pathway. Analysis of RNAi BES1 roots indicated that the BR-mediated QC divisions are downstream of BES1 (Figure 4). First, we observed that BR-mediated QC divisions are downstream of BRI1 (Figures 4A–4D, and 4G–4J). However, the *bzr1*-D mutants showed mild QC defects and BZR1 expression could not be detected in the QC cells (Figures 4E, 4F, 4O, 4P, 4T–4V). We observed that only BES1 and not BZR1 became activated in the QC upon BL treatment (Figures 4Q–4V), supporting a predominant role of BES1 in BR-mediated QC divisions. To unveil the regulation of QC divisions by both BES1 and BRAVO, we generated *bri1-116/bravo* and *bravo/bes1-D* double mutants. The absence of QC divisions in *bri1-116/bravo* double mutants, like in *bri1* mutants, pointed to the requirement of BR signaling in order to promote QC divisions (Figures 3N, 3O, and 4). In addition, the stronger QC division phenotype in *bravo/bes1-D* mutant compared to the single mutants (Figures 3L and 3O) indicates that BES1 and BRAVO do not regulate QC divisions in a linear pathway. In the same direction, local expression of BES1 in the QC cells in pWOX5::BES1-D-GFP displayed a stronger phenotype than *bravo* mutants (Figure 3M). Together, these data suggest that QC divisions are both activated by BES1 and repressed by BRAVO to preserve quiescence in the root meristem.

Biological Significance of the BRAVO Pathway in Root Development

In the stem cell niche, the activation of stress-associated BR-signaling triggers increased QC division and premature stem cell differentiation that results in aberrant root growth (González-García et al., 2011; Heyman et al., 2013). Our data indicate that BRAVO acts as a highly regionalized repressor, counteracting BR-mediated divisions in the QC. To further investigate its role as a repressor of cell division, we expressed BRAVO outside its native expression domain by generating inducible BRAVO lines. Ectopic induction of BRAVO led to a 50% reduction in root length of 6-day-old seedlings and a reduction of the meristematic cell number (Figures 5A–5D). Furthermore, this induction led to a significant deregulation of widely expressed cell cycle regulators such as *CYCB1;2*, *CYCD3;3*, *CYD2;2*, *RBR, KRP1*,

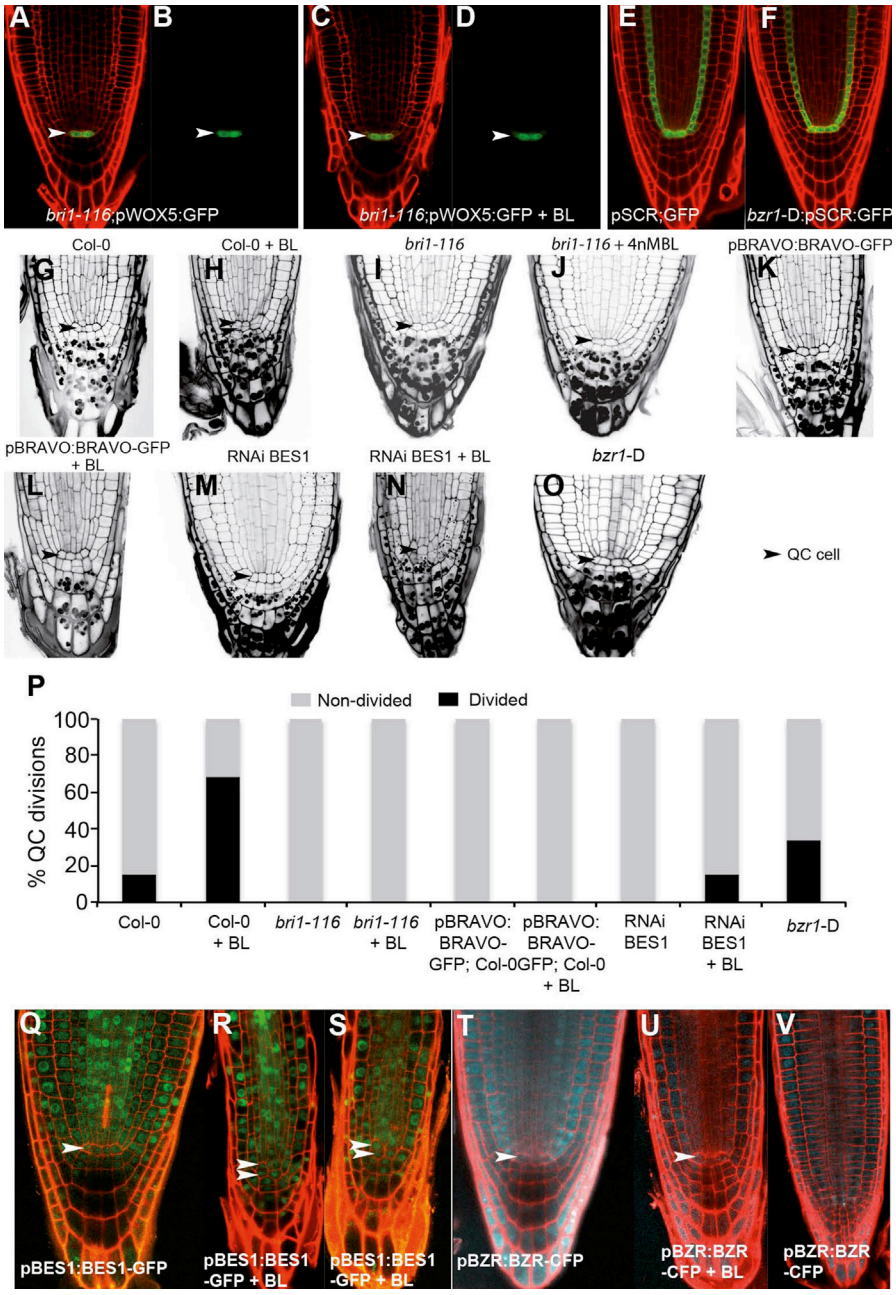

Figure 4. BR-Mediated QC Divisions Are Downstream of BES1

(A–F) Six-day-old seedlings counterstained with PI.

(A and B) *bri1-116;pWOX5:GFP*.

(C and D) *bri1-116;pWOX5:GFP* treated with BL continuously.

(E) pSCR:GFP expression.

(F) bzr1-D;pSCRGFP.

(G–O) Six-day-old seedlings mPS-PI stained of the indicated genotypes.

(P) Quantitative analysis of QC divisions.

(Q–V) Six-day-old seedlings counterstained with PI.

(Q) pBES1:BES1-GFP.

(R and S) pBES1:BES1-GFP after continuous BL treatment.

(T) pBZR:BZR-CFP.

(U) pBZR:BZR-CFP after continuous BL treatment.

(V) pBZR:BZR-CFP expression in the root epidermis. Note that BES1 is expressed in the QC cells, whereas there is no detectable expression of BZR.

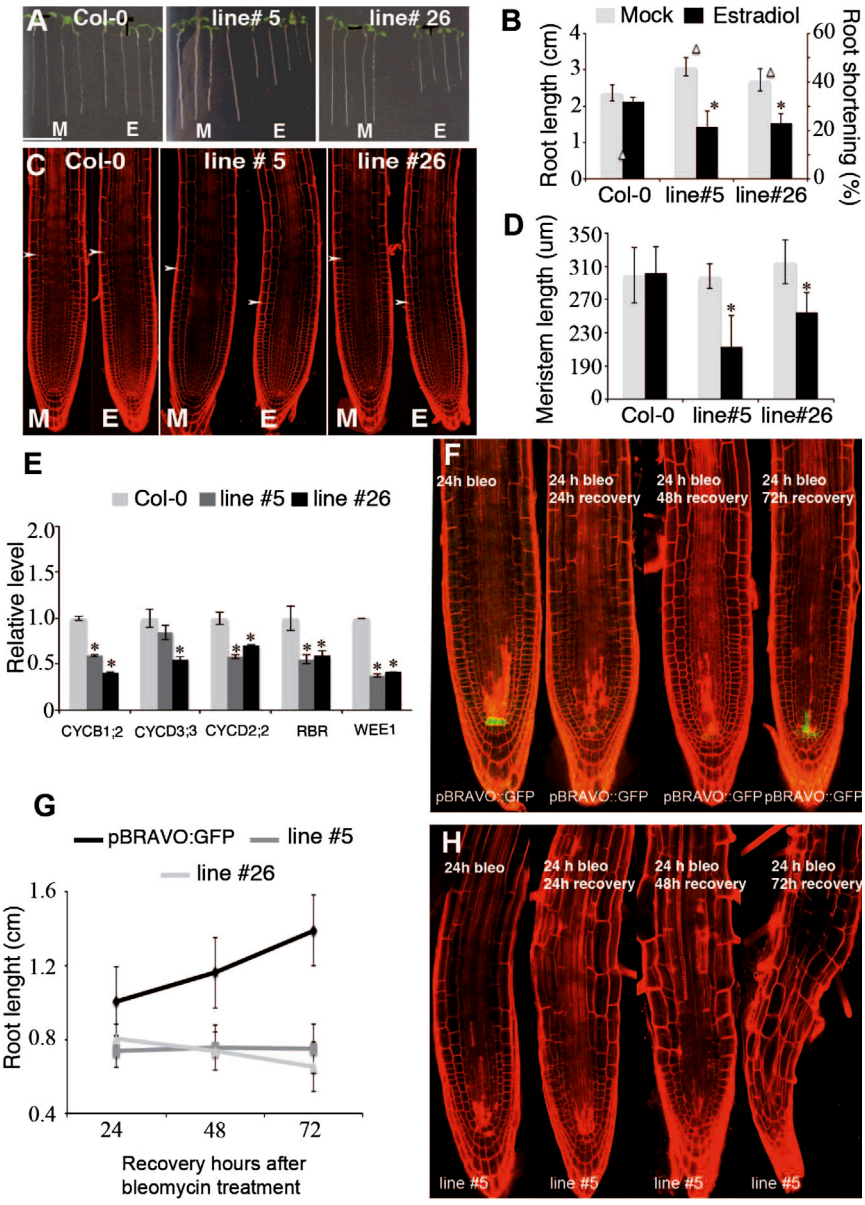

Figure 5. Ectopic *BRAVO* Expression Results in Reduced and Root Growth, and Organ Exhaustion upon DNA Damage

(A) Six-day-old seedlings of Col-0 and BRAVO estradiol inducible lines #5 and #26. M, mock; E, 20 μM estradiol.

(B) Root-length measurement of 6-day-old seedlings. Left y axis represents centimeters (bars), and right y axis represents the percentage of root shortening (triangles).

(C) Six-day-old roots of indicated genotypes counterstained with PI. White arrow represents the end of the meristematic zone.

(D) Quantification of meristem length in mock and estradiol-induced BRAVO lines.

(E) Relative levels of indicated cell cycle genes after induction of BRAVO overexpression.

(F) Expression of pBRAVO:GFP counterstained with PI, 4-day postgermination seedlings were treated with bleomycin for 24 hr (24 hr Bleo) and transfer to free-drug media after 24 hr (24 hr bleo, 24 hr recovery), 48 hr (24 hr bleo, 48 hr recovery), and 72 hr (24 hr bleo, 72 hr recovery).

(G) Root length after 24 hr bleomycin treatment.

(H) Ectopic expression of BRAVO, same treatments as (G).

*$p < 0.05$. Scale bar in (A) represents 1 cm. See also Figure S4.

KRP2, and *WEE1* (Figure 5E) concomitantly with *BRAVO* induction, in agreement with microarray data of BR-responsive genes (Figure S2). Thus, *BRAVO* can repress cell divisions by interfering with the normal cell cycle.

The continuous renewal of stem cells ensures proper root growth and development (Scheres, 2007). In light of our results, we hypothesized that BRAVO functions in conferring to the QC the capacity to overcome external stresses, i.e., DNA stress. Thus, using a radiolabeled drug, which promotes stem cell death by chemical induction of DNA damage (Cruz-Ramírez et al., 2013; Fulcher and Sablowski, 2009; Heyman et al., 2013), we investigated the role of *BRAVO* in controlling stem cell regeneration. Upon bleomycin treatment, WT plants expressing *pBRAVO:GFP* undergo a downregulation of BRAVO concomitantly with QC division. This indicates that BRAVO regulates the preceding QC division necessary to guarantee replenishment of the stem cell compartment and to promote root growth (Figures 5F and 5G). Moreover, BRs promoted DNA damage-mediated death of the QC cells and both *bes1D* and *bravo* mutants exhibited a reduced root growth recovery upon bleomycin treatment (Figure S4). In contrast, bleomycin treatment of plants that ectopically express *BRAVO* blocked root growth, and end up with organ exhaustion (Figures 5G and 5H). Hence, BR-mediated regulation of BRAVO functions to restrict quiescence and ensures the maintenance of regeneration potential of stem cells upon damage. Together, these analyses uncover a role for the BR-mediated BRAVO pathway in root development.

BRAVO and BES1 Module Creates a Switch in the QC Cells

Because both BRAVO and BES1 are found in QC cells and drive antagonistic effects on QC divisions in a nonlinear pathway, we evaluated whether they regulate each other to ensure a univocal response. First, we tested whether BES1 downregulation of BRAVO is transcriptional. Chromatin immunoprecipitation (ChIP) data showed that the dephosphorylated, active form of BES1 binds to the E-boxes of the BRAVO promoter (Figure 6A; Figure S1). This transcriptional repression was confirmed by transactivation assays in *Nicotiana benthamiana* and was released in the presence of BRAVO (Figures 1H and 6B). In addition, both ChIP and transactivation analysis revealed that

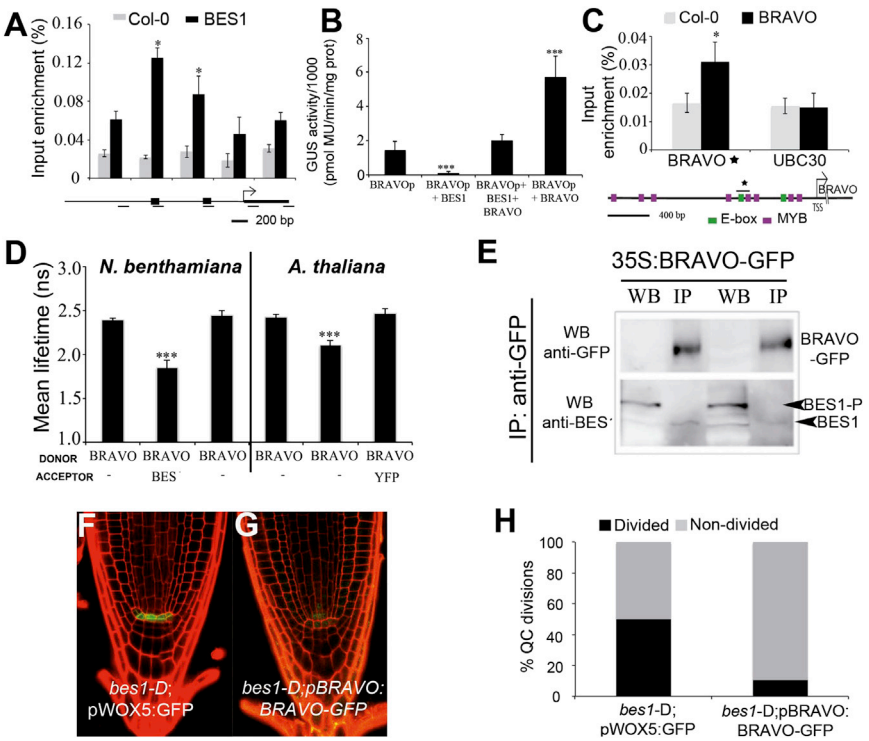

Figure 6. Mechanistic Basis for the BES1/BRAVO Signaling Module

(A) Input enrichment of BRAVO promoter containing E-boxes after ChIP-PCR; PCR fragments indicated in horizontal axis, E-boxes highlighted in black.

(B) Transient transactivation of *pBRAVO* by BES1 and BRAVO in *N. benthamiana* leaves.

(C) Input enrichment of *BRAVO* promoter containing E-boxes and MYB-boxes, bottom; schematic representation of BRAVO promoter containing both E-boxes and MYB-boxes. Star represents PCR fragments used in ChIP-PCR.

(D) Graphical representation of reduced CFP lifetime in nuclei coexpressing BRAVO-CFP (cyan fluorescence protein; donor) and BES1-YFP (yellow fluorescence protein; acceptor), as compared to nuclei expressing BRAVO-CFP alone; nuclear YFP was used as specificity control.

(E) Coimmunoprecipitation using 35S:BRAVO-GFP, top; enriched BRAVO-GFP protein complex after IP, bottom; BES1 dephosphorylated form (black arrow) is detected using anti-BES1 antibodies in the BRAVO-GFP protein immunoprecipitated fraction.

(F and G) Six-day-old seedlings counterstained with propidium iodide (PI) of the indicated genotypes.

(H) Quantification of QC divisions in (F) and (G). *, ***,$p < 0.05$ and < 0.001, respectively), error bars represent ± SEM. WB, western blot; IP, immunoprecipitation.

BRAVO binds to and promotes its own expression (Figures 6B and 6C), demonstrating that BRAVO can be transcriptionally regulated by both BRAVO and BES1.

The heterodimerization of BES1 with other MYB transcription factors has been reported (Yu et al., 2011). We next tested BRAVO/BES1 heterodimerization with fluorescence resonance energy transfer-fluorescence lifetime imaging microscopy (FRET-FLIM) and with coimmunoprecipitation experiments *in planta*. Our results showed that BRAVO interacts with the dephosphorylated, active form of BES1 in the nucleus (Figures 6D and 6E; Figure S4). To assess the biological activity of BRAVO/BES1 interaction, *bes1*-D; *pBRAVO::BRAVO-GFP* double mutants were generated. Increased levels of BRAVO suppressed the QC division phenotype of *bes1-D* (Figures 6F–6H), similar to the exogenous BL treatment of *pBRAVO::BRAVO-GFP* (Figures 4K, 4L, and 4P). In agreement, transactivation assays with BES1/BRAVO dimer suppress repression/activation activities of BES1 and BRAVO (Figure 6B), respectively. Altogether, these results show that BRAVO/BES1 proteins heterodimerize in the QC cells.

Finally, to understand how the cross-regulations between BES1 and BRAVO integrate the BR signaling that controls QC divisions, we built a mathematical model that takes into account the BRAVO-BES dimerization and *BRAVO* transcriptional control by BRAVO and BES1 (Figure 7A, see Mathematical Model within Experimental Procedures). Computational simulations predicted that these interactions drive robustly opposite amounts of BRAVO and active BES1 with a switch-like response to BR signaling (Figures 7B and S5). Specifically, a high amount of free BRAVO arises concomitantly with low amounts of free active BES1 (i.e., [HIGH, LOW] state) at low BR signaling (i.e., low BES1 dephosphorylation rates). As BR signaling increases, a switch (i.e., sharp transition) to an opposed state with strong free active BES1 and no free BRAVO (i.e., [LOW, HIGH] state) occurs. Taking into account the roles of BES1 and BRAVO in QC divisions unveiled by the mutant analyses, the (HIGH, LOW) state drives quiescence, whereas QC divisions are induced in the (LOW, HIGH) state. Together, these results provide a fine mechanism for BR-controlled QC divisions.

Parameter space exploration of the mathematical model indicated that the physical interaction between BES1 and BRAVO is crucial to drive opposed states of BRAVO and BES1 and a sharp transition (Figures 7C and S5). This is in agreement with the known ultrasensitive responses driven by molecular titration through heterodimer formation (Buchler and Louis, 2008; Cross and Buchler, 2009). In addition, our computational results show that the functional role of the BRAVO-BES1 heterodimer in *BRAVO* transcription is not relevant for these features to hold (Figure 7D). Moreover, BES1 transcriptional repression of *BRAVO* and *BRAVO* auto-activation facilitate that this sharp transition becomes bistable (Figure S5).

Importantly, the states of BRAVO and dephosphorylated BES1 expression predicted by the model are in agreement with the extent of BRAVO and dephosphorylated BES1 in the QC of WT plants and in plants treated with BL (Figures 1C–1E and 4). We next evaluated whether an abrupt switch in *BRAVO* expression with BR signaling occurs in vivo, as predicted by the model. To this end, we quantified *pBRAVO:GFP* fluorescence in individual QC cells after continuous BL treatments,

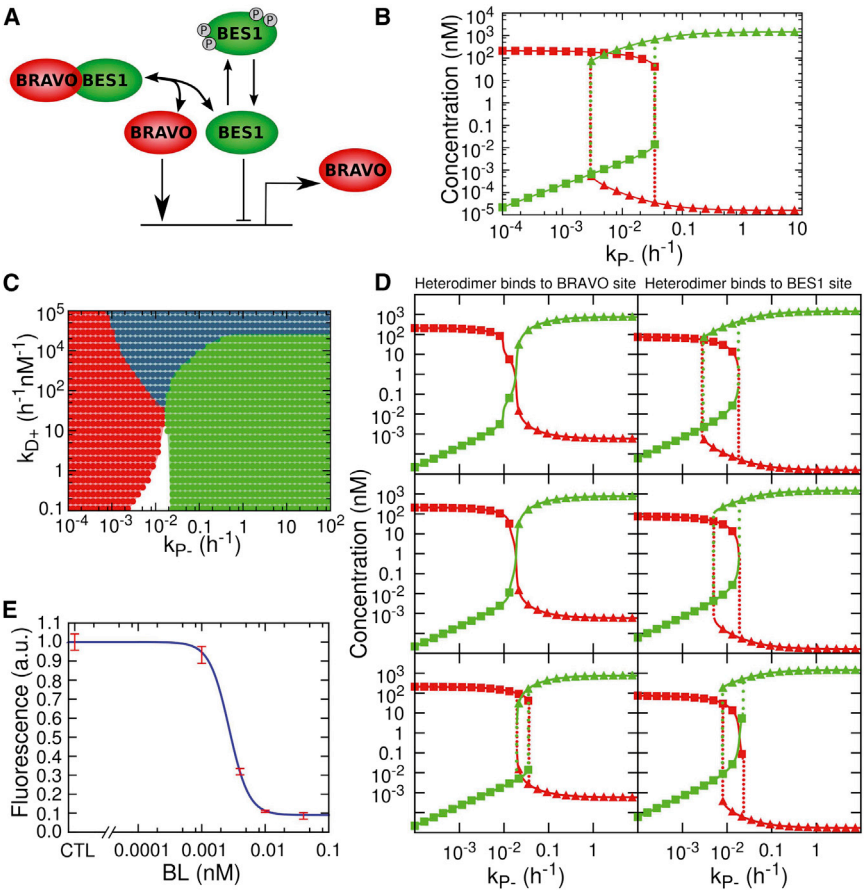

Figure 7. BES1/BRAVO Interaction Defines a Switch that Controls QC Divisions in the Root Apex

(A) Schematics of the reactions considered in the model. Blunt arrow stands for transcriptional repression. Production of BES1 and degradation of all molecules are omitted for simplicity.

(B) Amounts of free BRAVO (red) and free dephosphorylated BES1 (green) as a function of the BES1 dephosphorylation rate $k_{P\_}$. When free BRAVO is at high amounts, free dephosphorylated BES1 is almost absent. We term this state as (HIGH, LOW) (squares). Similarly, when BRAVO is absent, active dephosphorylated BES1 is at high amounts. We term this state (LOW, HIGH; triangles). The dephosphorylation rate controls a switch between these two states. Lines with symbols represent the stationary stable solutions of Equation 2 in Experimental Procedures. Parameter values are detailed in the Experimental Procedures.

(C) Bistable (dark blue) and monostable (red for [HIGH, LOW] and green for [LOW, HIGH]) regions in the parameter space of the BRAVO-BES1 dimerization rate (k_{D+}) and dephosphorylation rate ($k_{P\_}$). White represents those regions where the amounts of free BRAVO and free dephosphorylated BES1 differ in less than one order of magnitude. Other parameter values as in (B).

(D) As in (B), but when the BRAVO-BES1 heterodimer is functional, for different scenarios: (left) the heterodimer binds to the DNA at the BRAVO binding site (Equations 1 and 3); (right) the heterodimer binds to the DNA at the BES1 binding site (Equations 1 and 4); the heterodimer (top) represses, (middle) drives at basal rate, or (bottom) activates *BRAVO* transcription when it is the only element bound to the promoter. Parameter values as in (B) with (left) $K_{C1} = K_M$ and (top) $\varepsilon_{1C} = 0.1$, (middle) $\varepsilon_{1C} = 1$, (bottom) $\varepsilon_{1C} = \varepsilon_1 = 3.9$; (right) $K_{C2} = K_B$; and (top) $\varepsilon_{2C} = \varepsilon_2 = 0.068$, (middle) $\varepsilon_{2C} = 1$, (bottom) $\varepsilon_{2C} = 2$.

(E) *pBRAVO:GFP* expression in QC cells as a function of BL concentration. The dots indicate the mean fluorescence per QC cell averaged over n ($18 < n < 100$) QC cells of 6-day-old seedlings continuously treated at each indicated concentration of BL. Data from two experiments. SEM is indicated. Fluorescence (in arbitrary units) has been normalized to the CTL average fluorescence. The curved line represents the function $y = 1 - 0.91x^h/(x^h+0.0027^h)$ with $h = 2.8$ and x is the BL concentration, denoting the ultrasensitive response ($h > 1$) of *pBRAVO:GFP* expression to BL.

See also Figure S5.

uncovering that *BRAVO* displays an ultrasensitive response to BRs (Figure 7E).

DISCUSSION

BRs play key roles in cell division associated to developmental programs such as root meristem, the formation of organ boundaries, and stomata patterning, yet BR components operating at a cellular scale have not been disclosed. Our data unveil how BR signaling operates with cellular resolution, and defines BRAVO as a molecular repressor counteracting steroid-mediated divisions in the stem cell niche. This mechanism ensures the low rates of cell proliferation in the QC, whereas the behavior of the BRAVO/BES1 signaling module can confer the QC cells with the plasticity to adapt to environmental changing conditions. Collectively, our results support that BRAVO is a master regulator of cellular quiescence in plants.

The identification of *BRAVO* as the single gene appearing in a Venn diagram in a search for stem cell-specific BR-signaling components using FACS coupled to transcriptomics hinted at the potential significance of this locus. Despite that, *BRAVO* gene belongs to a large multigene family, *MYB* transcription factors (Dubos et al., 2010), the *bravo* knockout mutants exhibit cell-specific defects at the quiescent center cells of the root stem cell niche.

The regulation of quiescence in the stem cell niche, where the quiescent cells are surrounded by rapidly dividing stem cells, has been an outstanding question in developmental biology (Hsu and Fuchs, 2012; Morrison and Spradling, 2008). In the plant root, the quiescent cells provide short-range signals to maintain stemness of the surrounding cells (van den Berg et al., 1997). Our findings represent a major step forward in the present understanding of how steroids control stem cell division in eukaryotes. The positive actions of steroids on stem niches are well established across phyla (Ables and Drummond-Barbosa, 2010; Simões and Vivanco, 2011), including mammals, and excessive activation may result in pathologies such as breast or prostate cancer (Risbridger et al., 2010). However, little is known about negative

regulators that maintain homeostasis and the long-term function of stem cell niches. In this context, the identification of a negative regulator, BRAVO, that inhibits the steroid hormonal pathway of the root stem niche will serve as a paradigm that will be of relevance for other stem cell niches, beyond the root.

We propose that BRAVO negatively regulates QC divisions by acting as a safe-lock to retain QC cells in a mitotically inactive status. The lack of BRs signaling in the nondividing QC cells is supported by (1) the specific BRAVO expression, and (2) the lack of BRs-promoted ERF115 expression (Heyman et al., 2013), which suggests that the activation of the BR-signaling pathway is detrimental for proper QC function. This notion is further supported by radiolabeled drug treatment of BR-signaling mutants (Figure S4). Importantly, BRAVO dynamics upon DNA damage suggest its involvement in promoting quiescence, ensuring proper root growth regeneration. Oppositely, BRAVO downregulation would release the BR-dependent ERF115 expression (Heyman et al., 2013). QC cells are a reservoir of both auxin transport and biosynthesis (Overvoorde et al., 2010). Despite any specific quantification of BRs in planta has been carried out, it is attractive to speculate that low levels of BRs in the QC will result in low proliferation activities. Understanding the hierarchy of those among other regulators will further refine our understanding of quiescence.

Cell response to stimuli is fundamental for proper plant adaptation to environmental cues, and these reversible responses account for its renowned plasticity (Siegal-Gaskins et al., 2011). QC cells divide upon stimulation by hormones (González-García et al., 2011; Ortega-Martínez et al., 2007; Zhang et al., 2010, 2013), stem cell damage (Heyman et al., 2013), or cell cycle interference (Cruz-Ramírez et al., 2013) enabling replenishment of the stem cells upon damage. To preserve the QC function as a reservoir of stem cells, this transition between divided and nondivided QC cells should be reversible. Our mathematical modeling taking into account BES1/BRAVO mutual interaction, BRAVO autoactivation, and *BRAVO* transcriptional inhibition by BES1 results in a robust response to stimuli that is switch-like and is accompanied by opposed expressions of BRAVO and BES1. When considering that BRAVO and BES1 can both antagonistically regulate QC divisions, this switch-like response becomes relevant to ensure univocal responses on whether the QC needs to divide. Although alternative mechanisms driving switch-like responses cannot be discarded, we found that with BR hormone stimulation, BRAVO switches its expression in vivo sharply, thereby enabling the change from quiescence to the induction of QC divisions. Notably, the three elements involved in BRAVO and BES1 cross-regulation—(1) dimerization of two proteins, (2) transcriptional autoactivation of one of them, and (3) transcriptional repression by the other protein drive bistable cellular responses as shown with in silico evolutions of genetic circuits (François and Hakim, 2004). In agreement, our modeling results indicated that the sharp transition of BRAVO expression with BR signaling can robustly involve bistability of BRAVO expression states. The mechanism provided by the BES1/BRAVO signaling module gives a fine example for a selective control of cellular quiescence in eukaryotes.

EXPERIMENTAL PROCEDURES

Plant Material

Arabidopsis thaliana (L.) Heyhn, was in Columbia-0 (Col-0) background. To avoid ecotype variability, the *bes1-D* mutant, originally in Enkheim-2 (En-2) background was introgressed into Col-0 ecotype, all other lines were in Col-0 background. Marker lines used: *pBRAVO:GFP* (Lee et al., 2006), *pBRAVO:BRAVO-GFP* (Lee et al., 2006), *pWOX5:GFP* (Sarkar et al., 2007), *pAGL42:GFP* (Nawy et al., 2005), *pWOL:GFP*, *DR5:GFP* (Sabatini et al., 1999, 2003), and *pARF7:3GFP* (Rademacher et al., 2011; Wachsman et al., 2011). Mutant lines; *bravo* mutant lines were ordered from the SALK collection; *bravo-1* (SALK_060289), and *bravo-2* (SALK_062413). Other mutant lines: *bri1-116* (Li and Chory, 1997). Beta estradiol from Sigma diluted in DMSO was used to induce *BRAVO* expression. Bleomycin treatments (0.6 μg/ml) was performed for 24 hr, subsequently seedlings were imaged and transferred to half MS to follow root recovery.

Cell-Specific Transcriptomics

Protoplasts from specific tissues using pWOL:GFP and pAtHB15:YFP markers were sorted by FACS, and RNA from sorted cells was hybridized to the Affymetrix ATH1 GeneChip as described elsewhere (Birnbaum et al., 2005). Six-day-old roots grown in vertical plates were transferred to plates with half MS media supplemented with 10 nM BL at different times (0, 0.5, 1, 2, and 4 hr). Protoplasts were extracted in a Petri dish containing 0.5 mM $CaCl_2$, 0.5 mM $MgCl_2$, 5 mM MES, 1.5% Cellulase RS, 0.03% Pectolyase Y23, 0.25% BSA, at pH 5.5 with gentle agitation for 2 hr at room temperature until root cell protoplasts were released. Osmolarity was adjusted to 550 mmol/kg by the addition of D-sorbitol. The protoplast suspension was filtered through a nylon mesh (30 μm), washed several times, and resuspended with basic medium at 70 revolutions per minute. Subsequently, cells were purified with a multiparameter cell sorter. GFP fluorescent (530/30 nm) plots were compared to red autofluorescent (580/30 nm) to set gates around GFP-positive (GFP^+) and GFP-negative (GFP^-) cells. Sorted cells were resuspended into lysis buffer for RNA isolation.

Microarray Analysis

Normalized gene expression mean values were used to prepare input files for the GiTools analysis. For each gene at different points in *WOL* or 2 hr in *ATHB15*, the mean expression value was compared with the mean value of the untreated control and a p value was calculated in accordance. GiTools input files for up- and downregulated genes were prepared in the binomial format. When the ratio of the mean expression values between treated and untreated control was higher or lower than 1 and the p value was smaller than 0.05 or 0.01, then the gene was considered as up- or downregulated, respectively, at the specific point and assigned the value of "1" (presence). When the difference between gene expression mean value at a specific point versus the untreated control was not statistically significant ($p > 0.05$), then the gene was assigned a value of "0" (absence) for the specific point. GO enrichment analysis was performed using binomial distribution within the GiTools software. In this case, the probability of k genes in a particular GO category corresponds to the right tail of the following probability mass function: $f(k; n, p) = n!/[k!(n-k)!]^* pk^*(1-p)n-k$, where n is the number of genes in the GO category and p the proportion of genes in the category that are responsive to the treatment (López-Bigas et al., 2008).

Cloning

All clones where generated using Gateway technology from Invitrogen. BP recombination in both pDONOR221 and derivatives was used to generate entry clones. Primers used for cloning and genotyping are listed in Supplemental Information. Multisite Gateway technology allows us to create tissue-specific expression and LR recombination was used to generate destination vectors. pER8-GW destination vector was used to generate estradiol-inducible lines.

Chromatin Immunoprecipitation

For ChIP experiments, 6-day-old plants 35S:BES1-D-GFP and WT control plants were grown in half MS under long-day conditions for 6 days. Seedlings were fixed with 1% formaldehyde. Nuclei extraction was performed according to (Deal and Henikoff, 2011). ChIP experiments using anti-GFP antibodies

were performed according to (Gendrel et al., 2005). Detection of PCR products was performed using Absolute qPCR SYBR Green mix (Thermoscientific) in a Biorad termocycler. Three different biological replicates were performed for each region of interest. BRAVO ChIP were performed using 3 g of root tips expressing *pBRAVO:BRAVO-GFP* treated 5 days with 20 uM NPA; subsequent steps were conducted as BES1-D ChIP, and three biological replicates were performed.

Agrobacterium-Mediated Transient Assays

Agrobacterium-mediated transient expression assays in *N. benthamiana* leaves and *Arabidopsis* seedlings were performed as described elsewhere (Froidure et al., 2010).

Fluorescence Microscopy

Phenotypic analysis of roots of mPS-PI stained plants and GFP fluorescence were depicted as described (González-García et al., 2011). The CFP and YFP fluorescence in *N. benthamiana* and *Arabidopsis* epidermal cells was analyzed with a confocal laser scanning microscope (TCS SP2-SE; Leica) using a 63× water immersion objective lens (numerical aperture 1.20; PL APO). CFP fluorescence was excited with the 458 nm ray line of the argon laser and recorded in one of the confocal channels in the 465–520 nm emission range. YFP fluorescence was excited with the 514 nm line ray of the argon laser and detected in the range between 520 and 575 nm. Images were acquired in the sequential mode (20 Z plains per stack of images; 0.5 μm per Z plain) using Leica LCS software (version 2.61).

Fluorescence Lifetime Microscopy and Data Analysis

Fluorescence lifetime of the donor was experimentally measured in the presence and absence of the acceptor. FRET efficiency (E) was calculated by comparing the lifetime of the donor in the presence (τ_{DA}) or absence (τ_D) of the acceptor: $E = 1 - (\tau_{DA})/(\tau_D)$. Statistical comparisons between control (donor) and assay (donor + acceptor) lifetime values were performed with Student's t test. FRET-FLIM measurements were performed using a FLIM system coupled to a streak camera. The light source ($\lambda = 439$ nm) was a pulsed diode laser working at 2 MHz (Hamamatsu Photonics, Japan). All images were acquired with a 60× oil immersion lens (Plan Apo 1.4 numerical aperture, IR) mounted on an inverted microscope (Eclipse TE2000E, Nikon, Japan) coupled to the FLIM system. The fluorescence emission was directed back out into the detection unit through a band pass filter. The FLIM unit was composed of a streak camera (Streakscope C4334, Hamamatsu Photonics, Japan) coupled to a fast and high sensitivity CCD camera (model C8800-53C, Hamamatsu). For each nucleus, average fluorescence decay profiles were plotted and lifetimes were estimated by fitting data with tri-exponential function using a nonlinear least-squares estimation procedure.

Fluorimetric GUS Assays

For GUS reporter assays, the indicated constructs were transiently expressed in *N. benthamiana* leaves using *Agrobacterium*. Leaf discs were collected 36 hr after agroinoculation, frozen in liquid nitrogen and stored at −80°C until processing. After protein extraction, 1 μg of total protein was used in replicate to measure enzymatic activities of individual samples. GUS activity was measured using the substrate 4-methylumbelliferyl-β-D-glucuronidase as described (Froidure et al., 2010).

Coimmunoprecipitation

Approximately 2 g (1–2 leafs) were ground in liquid nitrogen using a mortar. The frozen, powdered material was transferred to a 50 ml falcon tube and 2 volumes (20 ml approx.) of extraction buffer was added (50 mM Tris/HCl, pH 7.5, 150 mM NaCl, 1% Triton X-100, and protease inhibitors PMSF, leupeptine, aprotinine, pepstatin A, and E-64). After thawing, the powdered material was homogenized by shaking. The resulting extract was left on ice for 20 min, followed by sonication (15 sec/paused/15 sec) three times at 10% of amplitude intensity, on ice. Samples were incubated 10 min on ice and subjected to centrifugation at 10,000 revolutions per minute two times for 10 min at 4°C. The resulting supernatant (17.5 ml) was incubated, under rotation at 4°C, with 75 μl of magnetic beads attached to anti-GFP antibodies (Miltenyi Biotec) for 1 hr. Magnetic beads with attached proteins were immobilized on a magnetic separator (MACS, Miltenyi Biotec) and washed two times with 200 μl extraction buffer. Bound proteins were eluted from the immobilized beads with 50 μl hot (95°C) SDS-PAGE loading buffer (1.6% SDS, 0.1 M dithiothreitol, 5% glycerol, 0.08 M TrisHCl pH 6.8, and bromophenol blue).

Eluted proteins were separated in 15% acrylamide SDS denaturing gel. Proteins were transferred to a nitrocellulose membrane (Hybonnd-ECL, GE Healthcare) by blotting 1 hr at 100 mV on ice under agitation. Membranes containing the immunoprecipitated proteins were blocked for 1 hr in 3% milk in PBS-T (0.1% Tween). One membrane was incubated with anti-GFP primary antibody for 1 hr and the other membrane was incubated with anti-BES1 primary antibody for 2.5 hr. Both membranes were incubated 1 hr in secondary antirabbit antibody.

Real-Time Analysis

RNA extraction of root tips from 6-day-old seedlings was performed using plant mini RNA extraction kit from QIAGEN following the manufacturer's instruction. cDNA synthesis was performed using QIAGEN superscript III, transcript level quantification in a Lightcycler 480 (Roche) using Sybrgreen and following the manufacturer's instructions. All primers are listed in Supplemental Information.

Mathematical Model

To model the BRAVO-BES1 interaction module, we considered that *BRAVO* transcription is repressed by dephosphorylated BES1 and activated by BRAVO, and that dephosphorylated BES1 and BRAVO form a heterodimer that is inactive (i.e., does not bind to the *BRAVO* promoter). We assumed: (1) transcription is independently controlled by BES1 and BRAVO, (2) BRAVO autoactivates itself in a noncooperative way and BES1 represses *BRAVO* noncooperatively too, (3) reversible dephosphorylation and phosphorylation of BES1, and (4) a constant production rate for phosphorylated BES1. From this, we obtained the following 17 reactions:

$$
\begin{aligned}
&D_1 + M \underset{k_{M-}}{\overset{k_{M+}}{\rightleftharpoons}} D_{1M}; \quad D_2 + B_d \underset{k_{B-}}{\overset{k_{B+}}{\rightleftharpoons}} D_{2B}\\
&D_1 + D_2 \xrightarrow{\alpha} D_1 + D_2 + M\\
&D_{1M} + D_2 \xrightarrow{\varepsilon_1 \alpha} D_{1M} + D_2 + M\\
&D_1 + D_{2B} \xrightarrow{\varepsilon_2 \alpha} D_1 + D_{2B} + M\\
&D_{1M} + D_{2B} \xrightarrow{\varepsilon_3 \alpha} D_{1M} + D_{2B} + M\\
&B \underset{k_{P+}}{\overset{k_{P-}}{\rightleftharpoons}} B_d\\
&M \xrightarrow{d_M} \varnothing\\
&\varnothing \xrightarrow{\beta} B \xrightarrow{d_B} \varnothing\\
&B_d \xrightarrow{d_{B_d}} \varnothing\\
&M + B_d \underset{k_{D-}}{\overset{k_{D+}}{\rightleftharpoons}} C \xrightarrow{d_C} \varnothing
\end{aligned}
\qquad \text{(Equation 1)}
$$

where the rates are indicated and all variables are concentrations of the following molecular species: M stands for free BRAVO; B for free phosphorylated BES1; B_d for free dephosphorylated (active) BES1; C for the BRAVO-dephosphorylated BES1 heterodimer; D_1 and D_2 stand for the free binding sites for BRAVO and dephosphorylated BES1, respectively, in the *BRAVO* promoter; and D_{1M} and D_{2B} correspond to these binding sites bound to BRAVO and dephosphorylated BES1, respectively. Rates for each reaction are indicated. Explicit mRNA dynamics with linear mRNA degradation and protein production proportional to mRNA concentration have been omitted for simplicity. Accordingly, the production rate of BRAVO protein α stands for the transcription rate times the translation rate over the *BRAVO* mRNA degradation rate. The deterministic stationary solutions computed do not depend on this simplification. α gives the production rate of BRAVO protein when the binding sites for BRAVO and dephosphorylated BES1 are free. Hereafter, we call this production rate the basal production rate. ε_1 is the ratio between the production rate of BRAVO when *BRAVO* is bound to its promoter over the basal production rate. Therefore, $\varepsilon_1 > 1$ stands for *BRAVO* auto-activation. ε_2 is the ratio between the BRAVO production rate when dephosphorylated BES1 is bound to the *BRAVO* promoter over the basal production rate. Notice that $\varepsilon_2 < 1$ stands for BES1 repression of *BRAVO* transcription. ε_3 is the ratio between the BRAVO production rate when both BRAVO and dephosphorylated BES1 are bound to the *BRAVO* promoter over the basal production rate. $\varepsilon_3 < 1$ and $\varepsilon_3 > 1$ stand for inhibition and activation, respectively, driven when both dephosphorylated

BES1 and BRAVO are bound to the *BRAVO* promoter, whereas $\varepsilon_3 = 1$ indicates that production is not modified from the basal one.

Using mass action kinetics, we can translate these reactions into the following six ordinary differential equations:

$$\begin{aligned}
&\dot{D}_1 = k_{M-} D_{1M} - k_{M+} M D_1; \quad D_1 + D_{1M} = D_{tot1}\\
&\dot{D}_2 = k_{B-} D_{2B} - k_{B+} B_d D_2; \quad D_2 + D_{2B} = D_{tot2}\\
&\dot{M} = \alpha(D_1 D_2 + \varepsilon_1 D_{1M} D_2 + \varepsilon_2 D_1 D_{2B} + \varepsilon_3 D_{1M} D_{2B}) + k_{M-} D_{1M}\\
&\quad + k_{D-} C - k_{M+} M D_1 - k_{D+} M B_d - d_M M\\
&\dot{B}_d = k_{p-} B + k_{B-} D_{2B} + k_{D-} C - k_{P+} B_d - k_{B+} B_d D_2 - k_{D+} M B_d - d_{B_d} B_d\\
&\dot{B} = \beta + k_{p+} B_d - k_{p-} B - d_B B\\
&\dot{C} = k_{D+} M B_d - k_{D-} C - d_C C
\end{aligned} \qquad \text{(Equation 2)}$$

Parameters $\varepsilon_1 = 3.9$, $\varepsilon_2 = 0.068$, $\varepsilon_3 = 1.353$, $K_M = k_{M+}/k_{M-} = 72.66\ \text{nM}^{-1}$, $K_B = k_{B+}/k_{B-} = 82.06\ \text{nM}^{-1}$, and $K_D = k_{D+}/k_{D-} = 164.76\ \text{nM}^{-1}$ were estimated from the experimental data of Figure 6B following the procedure described in the Supplemental Experimental Procedures. For all remaining nonfittable parameters, we chose their values within biologically reasonable ranges, setting: $D_{tot1} = D_{tot2} = 0.6$ nM, $\alpha = 3\ \text{nM h}^{-1}$, $\beta = 3\ \text{nM h}^{-1}$, $d_M = d_C = d_B = 0.02\ \text{h}^{-1}$, $d_{Bd} = 0.002\ \text{h}^{-1}$, $k_{P+} = 0.01\ \text{h}^{-1}$, and $k_{P-} = 0.002\ \text{h}^{-1}$. Because the stationary solutions depend also on k_{D+} and k_{D-}, we set them as $k_{D+} = 329.52\ \text{h}^{-1}\ \text{nM}^{-1}$, $k_{D-} = 2\ \text{h}^{-1}$ with $K_D = k_{D+}/k_{D-} = 164.76\ \text{nM}^{-1}$.

Mathematical Model with Active Heterodimer

To explore the possibility that the dephosphorylated BES1-BRAVO heterodimer could also transcriptionally regulate BRAVO, we considered two distinct scenarios, generating two different submodels. In the first one, the heterodimer binds to the same site in the *BRAVO* promoter as BRAVO itself with a binding constant $K_{C1} = k_{C1+}/k_{C1-}$ and drives *BRAVO* transcription at a rate ε_{C1} times the basal one. When both BES1 and the heterodimer are bound to the promoter, the transcription is modified by a factor ε_3, as when BRAVO is bound. These considerations give four new additional reactions to those in Equation 1:

$$\begin{aligned}
&D_1 + C \underset{k_{C1-}}{\overset{k_{C1+}}{\rightleftharpoons}} D_{1C}\\
&D_{1C} + D_2 \xrightarrow{\varepsilon_{1C}\alpha} D_{1C} + D_2 + M; \quad D_{1C} + D_{2B} \xrightarrow{\varepsilon_3\alpha} D_{1C} + D_{2B} + M
\end{aligned} \qquad \text{(Equation 3)}$$

The resulting dynamics from Equations 1 and 3 are obtained following the procedure used to obtain Equation 2. The stationary states of these dynamics were evaluated as described below for different parameter values of k_{C1+}, k_{C1-}, and ε_{C1}.

In the second scenario, the heterodimer binds to the binding site of BES1 with a binding constant $K_{C2} = k_{C2+}/k_{C2-}$ and activates or represses *BRAVO* transcription by a factor ε_{C2}. When both BRAVO and the heterodimer are bound to the promoter, the transcription is modified by a factor ε_3, as when BRAVO is bound. The corresponding reactions, which need to be added to those in Equation 1, are

$$\begin{aligned}
&D_2 + C \underset{k_{C2-}}{\overset{k_{C2+}}{\rightleftharpoons}} D_{2C}\\
&D_1 + D_{2C} \xrightarrow{\varepsilon_{2C}\alpha} D_1 + D_{2C} + M; \quad D_{1M} + D_{2C} \xrightarrow{\varepsilon_3\alpha} D_{1M} + D_{2C} + M
\end{aligned} \qquad \text{(Equation 4)}$$

The resulting dynamics from Equations 1 and 4 are obtained following the procedure used to obtain Equation 2. The stationary states of these dynamics were evaluated as described below for different parameter values of k_{C2+}, k_{C2-}, and ε_{C2}.

Mathematical Analysis of the Model

We obtained all the steady states of the above dynamics by setting the derivatives to 0 using Mathematica Software (Wolfram Research, Mathematica, Version 9.0). Solid lines with symbols in bifurcation diagrams denote the stable steady states found. Dashed lines in bifurcation diagrams are a guide to the eye for transitions. In parameter space explorations, solutions are computed at the center of the plotted points, and colored overlays are guides to the eye. Stability of the solutions was checked through numerical integration of the dynamics using custom-made software.

ACCESSION NUMBERS

The accession number for the microarray data is GEO: GSE67144.

SUPPLEMENTAL INFORMATION

Supplemental Information includes Supplemental Experimental Procedures, five figures, and two tables and can be found with this article online at http://dx.doi.org/10.1016/j.devcel.2014.05.020.

AUTHOR CONTRIBUTIONS

M.-P.G.-G. performed FACS and microarray experiments in the Benfey (P.N.B.) laboratory, and K.G.A. and N.L.-B. analyzed the microarray data. S.R. performed transactivation assays, and S.R. and A.J. performed FRET-FLIM assays. N.F.-V. carried out the coIP experiments. M.I. and D.F. performed mathematical modeling. J.V.-B. performed all the other experiments in the manuscripts. A.I.C.-D. conceived the project; and J.V.-B., M.I., and A.I.C.-D. designed experiments, analyzed the data, and wrote the manuscript.

ACKNOWLEDGMENTS

We acknowledge M.A. Blázquez, S. Mora-García, and M. Serrano for insightful comments on the manuscript; Y. Yin for anti-BES1 antibodies; X. Wang for RNAi BES1 lines; D. Weijers for ARF7:GFP seeds; and M. Amenós for confocal microscopy assistance. J.V.-B. and N.F.-V. are funded by FI PhD fellowship from the Generalitat de Catalunya (GC) in the A.I.C.-D. laboratory. J.V.-B. received a short-term fellowship (BE1-00924) in the Lohmann (J.U.L.) laboratory supported by the SFB873 of the DFG. Research by D.F and M.I. is funded by FIS2012-37655-C02-02 by the Spanish Ministry de Economy and Competitiveness and 2009SGR14 from GC, and D.F. has a PhD fellowship (FPU-AP2009-3736). S.R. is funded by the Laboratoire d'Excellence (LABEX) TULIP (ANR-10-LABX-41). M.-P.G.-G. received a "Juan de la Cierva" postdoctoral contract from the Spanish Ministry of Science in the Ana Caño (A.I.C.-D.) laboratory, and an HFSP short-term fellowship in the Benfey (P.N.B.) laboratory. P.N.B. is funded by NSF Arabidopsis 2010 grant. Work in the Ana Caño (A.I.C.-D.) laboratory is funded by a BIO2010/007 grant from the Spanish Ministry of Innovation and Science and a Marie-Curie Initial Training Network "BRAVISSIMO" (grant no. PITN-GA-2008-215118).

Received: March 17, 2014
Revised: May 9, 2014
Accepted: May 23, 2014
Published: June 26, 2014

REFERENCES

Ables, E.T., and Drummond-Barbosa, D. (2010). The steroid hormone ecdysone functions with intrinsic chromatin remodeling factors to control female germline stem cells in Drosophila. Cell Stem Cell *7*, 581–592.

Bell, E.M., Lin, W.-C., Husbands, A.Y., Yu, L., Jaganatha, V., Jablonska, B., Mangeon, A., Neff, M.M., Girke, T., and Springer, P.S. (2012). Arabidopsis lateral organ boundaries negatively regulates brassinosteroid accumulation to limit growth in organ boundaries. Proc. Natl. Acad. Sci. USA *109*, 21146–21151.

Birnbaum, K., Jung, J.W., Wang, J.Y., Lambert, G.M., Hirst, J.A., Galbraith, D.W., and Benfey, P.N. (2005). Cell type-specific expression profiling in plants via cell sorting of protoplasts from fluorescent reporter lines. Nat. Methods *2*, 615–619.

Brady, S.M., Orlando, D.A., Lee, J.-Y., Wang, J.Y., Koch, J., Dinneny, J.R., Mace, D., Ohler, U., and Benfey, P.N. (2007). A high-resolution root spatiotemporal map reveals dominant expression patterns. Science *318*, 801–806.

Buchler, N.E., and Louis, M. (2008). Molecular titration and ultrasensitivity in regulatory networks. J. Mol. Biol. *384*, 1106–1119.

Cheung, T.H., and Rando, T.A. (2013). Molecular regulation of stem cell quiescence. Nat. Rev. Mol. Cell Biol. *14*, 329–340.

Cross, F.R., and Buchler, N.E. (2009). msb200930. Mol. Syst. Biol. *5*, 1–7.

Cruz-Ramírez, A., Díaz-Triviño, S., Wachsman, G., Du, Y., Arteága-Vázquez, M., Zhang, H., Benjamins, R., Blilou, I., Neef, A.B., Chandler, V., and Scheres, B. (2013). A scarecrow-retinoblastoma protein network controls protective quiescence in the Arabidopsis root stem cell organizer. PLoS Biol. *11*, e1001724.

Deal, R.B., and Henikoff, S. (2011). The INTACT method for cell type-specific gene expression and chromatin profiling in Arabidopsis thaliana. Nat. Protoc. *6*, 56–68.

Dubos, C., Stracke, R., Grotewold, E., Weisshaar, B., Martin, C., and Lepiniec, L. (2010). MYB transcription factors in Arabidopsis. Trends Plant Sci. *15*, 573–581.

Fàbregas, N., Li, N., Boeren, S., Nash, T.E., Goshe, M.B., Clouse, S.D., de Vries, S., and Caño-Delgado, A.I. (2013). The brassinosteroid insensitive1-like3 signalosome complex regulates Arabidopsis root development. Plant Cell *25*, 3377–3388.

François, P., and Hakim, V. (2004). Design of genetic networks with specified functions by evolution in silico. Proc. Natl. Acad. Sci. USA *101*, 580–585.

Froidure, S., Canonne, J., Daniel, X., Jauneau, A., Brière, C., Roby, D., and Rivas, S. (2010). AtsPLA2-alpha nuclear relocalization by the Arabidopsis transcription factor AtMYB30 leads to repression of the plant defense response. Proc. Natl. Acad. Sci. U S A. *107*, 15281–15286.

Fulcher, N., and Sablowski, R. (2009). Hypersensitivity to DNA damage in plant stem cell niches. Proc. Natl. Acad. Sci. USA *106*, 20984–20988.

Gendrel, A.-V., Lippman, Z., Martienssen, R., and Colot, V. (2005). Profiling histone modification patterns in plants using genomic tiling microarrays. Nat. Methods *2*, 213–218.

Gendron, J.M., Liu, J.-S., Fan, M., Bai, M.-Y., Wenkel, S., Springer, P.S., Barton, M.K., and Wang, Z.-Y. (2012). Brassinosteroids regulate organ boundary formation in the shoot apical meristem of Arabidopsis. Proc. Natl. Acad. Sci. USA *109*, 21152–21157.

González-García, M.P., Vilarrasa-Blasi, J., Zhiponova, M., Divol, F., Mora-García, S., Russinova, E., and Caño-Delgado, A.I. (2011). Brassinosteroids control meristem size by promoting cell cycle progression in Arabidopsis roots. Development *138*, 849–859.

Gudesblat, G.E., Schneider-Pizoń, J., Betti, C., Mayerhofer, J., Vanhoutte, I., van Dongen, W., Boeren, S., Zhiponova, M., de Vries, S., Jonak, C., and Russinova, E. (2012). SPEECHLESS integrates brassinosteroid and stomata signalling pathways. Nat. Cell Biol. *14*, 548–554.

Hacham, Y., Holland, N., Butterfield, C., Ubeda-Tomas, S., Bennett, M.J., Chory, J., and Savaldi-Goldstein, S. (2011). Brassinosteroid perception in the epidermis controls root meristem size. Development *138*, 839–848.

Heyman, J., Cools, T., Vandenbussche, F., Heyndrickx, K.S., Van Leene, J., Vercauteren, I., Vanderauwera, S., Vandepoele, K., De Jaeger, G., Van Der Straeten, D., and De Veylder, L. (2013). ERF115 controls root quiescent center cell division and stem cell replenishment. Science *342*, 860–863.

Hsu, Y.-C., and Fuchs, E. (2012). A family business: stem cell progeny join the niche to regulate homeostasis. Nat. Rev. Mol. Cell Biol. *13*, 103–114.

Kim, T.-W., Michniewicz, M., Bergmann, D.C., and Wang, Z.-Y. (2012). Brassinosteroid regulates stomatal development by GSK3-mediated inhibition of a MAPK pathway. Nature *482*, 419–422.

Lee, J.-Y., Colinas, J., Wang, J.Y., Mace, D., Ohler, U., and Benfey, P.N. (2006). Transcriptional and posttranscriptional regulation of transcription factor expression in Arabidopsis roots. Proc. Natl. Acad. Sci. U S A. *103*, 6055–6060.

Li, J., and Chory, J. (1997). A putative leucine-rich repeat receptor kinase involved in brassinosteroid signal transduction. Cell *90*, 929–938.

López-Bigas, N., Kisiel, T.A., Dewaal, D.C., Holmes, K.B., Volkert, T.L., Gupta, S., Love, J., Murray, H.L., Young, R.A., and Benevolenskaya, E.V. (2008). Genome-wide analysis of the H3K4 histone demethylase RBP2 reveals a transcriptional program controlling differentiation. Mol. Cell *31*, 520–530.

Mähönen, A.P., Bonke, M., Kauppinen, L., Riikonen, M., Benfey, P.N., and Helariutta, Y. (2000). A novel two-component hybrid molecule regulates vascular morphogenesis of the Arabidopsis root. Genes Dev. *14*, 2938–2943.

Morrison, S.J., and Spradling, A.C. (2008). Stem cells and niches: mechanisms that promote stem cell maintenance throughout life. Cell *132*, 598–611.

Müssig, C., Shin, G.-H., and Altmann, T. (2003). Brassinosteroids promote root growth in Arabidopsis. Plant Physiol. *133*, 1261–1271.

Nawy, T., Lee, J.-Y., Colinas, J., Wang, J.Y., Thongrod, S.C., Malamy, J.E., Birnbaum, K., and Benfey, P.N. (2005). Transcriptional profile of the Arabidopsis root quiescent center. Plant Cell *17*, 1908–1925.

Ortega-Martínez, O., Pernas, M., Carol, R.J., and Dolan, L. (2007). Ethylene modulates stem cell division in the Arabidopsis thaliana root. Science *317*, 507–510.

Overvoorde, P., Fukaki, H., and Beeckman, T. (2010). Auxin control of root development. Cold Spring Harb. Perspect. Biol. *2*, a001537.

Rademacher, E.H., Möller, B., Lokerse, A.S., Llavata-Peris, C.I., van den Berg, W., and Weijers, D. (2011). A cellular expression map of the Arabidopsis AUXIN RESPONSE FACTOR gene family. Plant J. *68*, 597–606.

Risbridger, G.P., Davis, I.D., Birrell, S.N., and Tilley, W.D. (2010). Breast and prostate cancer: more similar than different. Nat. Rev. Cancer *10*, 205–212.

Sabatini, S., Beis, D., Wolkenfelt, H., Murfett, J., Guilfoyle, T., Malamy, J., Benfey, P., Leyser, O., Bechtold, N., Weisbeek, P., et al. (1999). An auxin-dependent distal organizer of pattern and polarity in the Arabidopsis root. Cell *99*, 463–472.

Sabatini, S., Heidstra, R., Wildwater, M., and Scheres, B. (2003). SCARECROW is involved in positioning the stem cell niche in the Arabidopsis root meristem. Genes Dev. *17*, 354–358.

Sarkar, A.K., Luijten, M., Miyashima, S., Lenhard, M., Hashimoto, T., Nakajima, K., Scheres, B., Heidstra, R., and Laux, T. (2007). Conserved factors regulate signalling in Arabidopsis thaliana shoot and root stem cell organizers. Nature *446*, 811–814.

Scheres, B. (2007). Stem-cell niches: nursery rhymes across kingdoms. Nat. Rev. Mol. Cell Biol. *8*, 345–354.

Siegal-Gaskins, D., Mejia-Guerra, M.K., Smith, G.D., and Grotewold, E. (2011). Emergence of switch-like behavior in a large family of simple biochemical networks. PLoS Comput. Biol. *7*, e1002039.

Simões, B.M., and Vivanco, M.D. (2011). Cancer stem cells in the human mammary gland and regulation of their differentiation by estrogen. Future Oncol. *7*, 995–1006.

Sun, Y., Fan, X.-Y., Cao, D.-M., Tang, W., He, K., Zhu, J.-Y., He, J.-X., Bai, M.-Y., Zhu, S., Oh, E., et al. (2010). Integration of brassinosteroid signal transduction with the transcription network for plant growth regulation in Arabidopsis. Dev. Cell *19*, 765–777.

van den Berg, C., Willemsen, V., Hendriks, G., Weisbeek, P., and Scheres, B. (1997). Short-range control of cell differentiation in the Arabidopsis root meristem. Nature *390*, 287–289.

Wachsman, G., Heidstra, R., and Scheres, B. (2011). Distinct cell-autonomous functions of RETINOBLASTOMA-RELATED in Arabidopsis stem cells revealed by the Brother of Brainbow clonal analysis system. Plant Cell *23*, 2581–2591.

Wang, Z.-Y., Nakano, T., Gendron, J., He, J., Chen, M., Vafeados, D., Yang, Y., Fujioka, S., Yoshida, S., Asami, T., and Chory, J. (2002). Nuclear-localized BZR1 mediates brassinosteroid-induced growth and feedback suppression of brassinosteroid biosynthesis. Dev. Cell *2*, 505–513.

Wilson, A., and Trumpp, A. (2006). Bone-marrow haematopoietic-stem-cell niches. Nat. Rev. Immunol. *6*, 93–106.

Yin, Y., Wang, Z.-Y., Mora-Garcia, S., Li, J., Yoshida, S., Asami, T., and Chory, J. (2002). BES1 accumulates in the nucleus in response to brassinosteroids to regulate gene expression and promote stem elongation. Cell *109*, 181–191.

Yu, X., Li, L., Zola, J., Aluru, M., Ye, H., Foudree, A., Guo, H., Anderson, S., Aluru, S., Liu, P., et al. (2011). A brassinosteroid transcriptional network revealed by genome-wide identification of BESI target genes in Arabidopsis thaliana. Plant J. *65*, 634–646.

Zhang, H., Han, W., De Smet, I., Talboys, P., Loya, R., Hassan, A., Rong, H., Jürgens, G., Paul Knox, J., and Wang, M.-H. (2010). ABA promotes quiescence of the quiescent centre and suppresses stem cell differentiation in the Arabidopsis primary root meristem. Plant J. *64*, 764–774.

Zhang, W., Swarup, R., Bennett, M., Schaller, G.E., and Kieber, J.J. (2013). Cytokinin induces cell division in the quiescent center of the Arabidopsis root apical meristem. Curr. Biol. *23*, 1979–1989.

Zhiponova, M.K., Vanhoutte, I., Boudolf, V., Betti, C., Dhondt, S., Coppens, F., Mylle, E., Maes, S., González-García, M.P., Caño-Delgado, A.I., et al. (2013). Brassinosteroid production and signaling differentially control cell division and expansion in the leaf. New Phytol. *197*, 490–502.